JOURNAL OF COMPUTATIONAL PHYSICS 23, 393–403 (1977)

The Korteweg–de Vries–Burgers Equation

JOSÉ CANOSA* AND JENÖ GAZDAG

IBM Scientific Center, Palo Alto, California 94304

Received June 11, 1976; revised July 30, 1976

The time evolution and stability of the shock solutions of the Korteweg–de Vries–Burgers equation are studied numerically. It is found that nonanalytic initial data satisfying the boundary conditions of the problem evolve asymptotically into the steady-state shocks predicted by a time-independent analysis. Like Burgers' equation, the Korteweg–de Vries–Burgers equation has a unique shock profile; this analogy suggests that the Korteweg–de Vries–Burgers shocks are stable against small perturbations, while the numerical experiments suggest further that the shocks are stable even when subject to large perturbations.

1. INTRODUCTION

We present a study of the Korteweg–de Vries–Burgers (KdVB) equation in the form

$$u_t + 2uu_x - \nu u_{xx} + \mu u_{xxx} = 0, \qquad \nu > 0, \qquad \mu > 0. \tag{1}$$

This is a nonlinear partial differential equation incorporating damping and dispersion which was derived by Su and Gardner [1] for a wide class of nonlinear systems in the weak nonlinearity and long-wavelength approximations. The steady-state solutions of (1) were studied by Grad and Hu [2] in the context of weak plasma skocks propagating perpendicularly to a magnetic field; in particular, they carried out a phase-plane analysis which showed that when diffusion dominates dispersion the steady-state solutions of (1) are monotonic shocks, and when dispersion dominates the shocks are oscillatory. Johnson [3] discussed (1) in a study of wave propagation through liquid-filled elastic tubes; subsequently he found that (1) was also useful for the description of shallow water waves on a viscous fluid [4]. More recently, Hu [5] has obtained (1) when including electron inertia effects in the description of weak nonlinear plasma waves. The previous work dealt with the steady-state solutions of (1). The aim of this work is to gain a more complete knowledge of the KdVB equation by studying the time evolution of its solutions, and the stability of the steady states.

In Section 2, we discuss the steady-state solutions of (1). When diffusion dominates dispersion, the steady-state solution is a monotonic shock whose profile is given with very high accuracy by a second-order asymptotic solution. When dispersion dominates, the steady-state solution is a shock which is oscillatory upstream and monotonic downstream. The time-dependent numerical solutions given in Section 3 show the evolution of nonanalytic initial data to the steady-state solutions predicted by the

* Present address: ITT Laboratories of Spain, Av. America km. 7, 2, Madrid 27, Spain.

ISSN 0021-9991

time-independent analysis. The numerical experiments suggest that the KdVB shocks are stable against large perturbations in their waveforms.

2. Steady-State Solutions

In this section, we review the properties of the steady-state solutions of the KdVB equation. In particular, we give a highly accurate second-order asymptotic solution for the monotonic shock profile. We emphasize that for fixed dispersion and diffusion coefficients μ and ν, and fixed upstream ($x \to -\infty$) and downstream ($x \to +\infty$) values of the distribution, the steady-state solutions of (1) have a unique profile. In this respect, the KdVB equation is similar to Burgers' equation [6, 7] where the shock profile is also unique, and different from the Korteweg–de Vries (KdV] equation [8] and Fisher's equation [9], where for fixed upstream and downstream values of the distribution there is a one-parameter family of steady-state profiles. This analogy with Burgers' equation suggests that the KdVB shocks are stable against waveform perturbations [10], and this is supported by the results of the numerical experiments in Section 3.

In this paper we are interested in the solutions of Eq. (1), such that all their x derivatives tend to zero as $x \to \pm\infty$, and that satisfy the upstream and downstream boundary conditions

$$\lim_{x \to -\infty} u(x, t) = u_{-\infty} = 1, \qquad t \geqslant 0, \tag{2a}$$

$$\lim_{x \to +\infty} u(x, t) = u_{+\infty} = 0, \qquad t \geqslant 0, \tag{2b}$$

where for convenience and without loss of generality the upstream value $u_{-\infty}$ has been chosen as unity, and the downstream value as zero. The equation for the steady-state solutions is obtained by assuming traveling wave solutions of Eq. (1) of the form

$$u(x, t) = u(x - ct - x_0) \equiv u(s), \tag{3}$$

where c is the wave propagation speed and x_0 is an arbitrary constant. Substitution of Eq. (3) into Eq. (1) gives a nonlinear ordinary differential equation for the steady-state solutions,

$$-c(du/ds) + 2u(du/ds) - \nu(d^2u/ds^2) + \mu(d^3u/ds^3) = 0. \tag{4}$$

One integration with respect to s gives

$$-cu + u^2 - \nu(du/ds) + \mu(d^2u/ds^2) = A. \tag{5}$$

The downstream condition Eq. (2b) together with the fact that all s derivatives are zero for $s \to \pm\infty$ determine the integration constant

$$A = -cu_{+\infty} + u_{+\infty}^2 = 0. \tag{6}$$

The upstream condition Eq. (2a) and the fact that all s derivatives vanish as $s \to \pm\infty$ give

$$u_{-\infty}(u_{-\infty} - c) = 0 \tag{7}$$

or

$$c = u_{-\infty} = 1. \tag{8}$$

Equations (5) through (8) show that there is a unique value of c and a corresponding solution of Eq. (5) that satisfy all the conditions of our problem. This solution gives the profile of a shock wave that propagates with a velocity equal to the upstream value of u (see Eq. (8)). Because x_0 in Eq. (3) is an arbitrary constant, any arbitrary space translation of the shock wave results also in a solution of (1); in other words, the steady-state solutions of (1) are invariant to space translation. This result is similar to that obtained for Burgers' equation, where the upstream and downstream values also determine a unique shock-wave profile and its propagation speed. The result (8) is in contrast with those obtained for the KdV equation and Fisher's equation. In KdV's equation [8] for $u \to 0$ as $x \to \pm\infty$, there is a one-parameter family of steady-state profiles (solitons) with propagation speeds $c > 0$; in the case of Fisher's equation [9], for $u \to 1$ as $x \to -\infty$ and $u \to 0$ as $x \to +\infty$, there is also a one-parameter family of steady-state profiles with propagation speeds $c \geqslant 2$.

The steady-state equation (5), where $A = 0$ (see (6)), with the proper boundary conditions consistent with (2a) and (2b) is

$$\begin{gathered} \mu(d^2u/ds^2) - \nu(du/ds) - u + u^2 = 0, \\ u(-\infty) = 1, \qquad u(+\infty) = 0. \end{gathered} \tag{9}$$

Grad and Hu [2] showed that the dissipative effects dominate over the dispersive effects when

$$\nu^2 \geqslant 4\mu. \tag{10}$$

In this case the solution of (9) is a shock decreasing monotonically from the upstream to the downstream value of u. If

$$\nu^2 < 4\mu, \tag{11}$$

the dispersive effects dominate over the dissipative effects; in this case, the shock becomes oscillatory upstream and monotonic downstream.

When (10) holds, it is convenient to introduce the new independent and dependent variables

$$z = -s/\nu, \qquad y = 1 - u, \tag{12}$$

so that (9) becomes

$$\begin{gathered} \epsilon(d^2y/dz^2) + dy/dz + y - y^2 = 0, \\ y(-\infty) = 1, \qquad y(+\infty) = 0, \qquad \epsilon \equiv \mu/\nu^2 \leqslant \tfrac{1}{4}, \end{gathered} \tag{13}$$

which is identical to Eq. (20) of [9] giving the traveling wave solutions of Fisher's equation. The asymptotic solution of (13), given by Eq. (25) of [9], is now transformed taking into account the change of variables (12). In this way, we obtain the asymptotic solution of (9), valid when the condition (10) holds:

$$u(s;\epsilon) = \frac{1}{1+\exp(s/\nu)} + \epsilon\frac{\exp(s/\nu)}{[1+\exp(s/\nu)]^2} \times \left(1 - \ln\frac{4\exp(s/\nu)}{[1+\exp(s/\nu)]^2}\right) + O(\epsilon^2), \tag{14}$$

$$\epsilon \equiv \mu/\nu^2 \leqslant \tfrac{1}{4}.$$

Equation (14) gives all the monotonic shock profiles of the KdVB equation with excellent accuracy, even for the case when the expansion parameter $\epsilon \equiv \mu/\nu^2$ has its maximum value $\frac{1}{4}$ [9].

Johnson's main interest and achievement [3] was to obtain an asymptotic solution for the oscillatory shock defined by (9) in the strong dispersion limit (see (11)) $\nu^2 \ll 4\mu$, which is the opposite from the one we obtained, valid for $\nu^2 \geqslant 4\mu$. He also dealt very briefly with the problem of obtaining a second-order asymptotic solution for the monotonic shock profile ($\nu^2 \geqslant 4\mu$). However, his second-order result is incorrect in two respects. A trivial one is that the integration giving his second-order term is incorrect; somewhat more important, he did not determine the integration constant by using the proper conditions [9]. As a consequence, even when corrected for the mistake in the integration, his result (which is obtained from (14) substituting the one before the logarithmic term in the last parentheses by a zero) is not better than the first-order result in the vicinity of the point of inflection of the shock. In [9], we showed that the proper determination of the integration constant necessary to obtain (14) required the knowledge of the height and slope of the point of inflection of the shock profile in the physical plane. These are (see [9, Eq. (15)] after taking into account the change of variables (12) and the definition of ϵ in (13))

$$(u, du/ds) = [\tfrac{1}{2} + \epsilon/4, -(1 - \epsilon^2/4)/4\nu]. \tag{15}$$

The steepness of the shock given by $|du/ds|$ in (15) is to second-order accuracy in ϵ

$$S = \tfrac{1}{4}\nu + O(\epsilon^2). \tag{16}$$

This result shows that for the monotonic shocks, the steepness, which might be considered a measure of the shock strength, is inversely proportional to the diffusion coefficient, and, to second-order accuracy, independent of the dispersion coefficient. As the second-order solution (14) is highly accurate, this means that, as long as (10) holds, the shock strength is practically independent of the dispersion coefficient. Indeed, diffusion greatly dominates dispersion.

When condition (11) holds, the shock strength is so large that the shock becomes oscillatory upstream [2, 3]. In the limit $4\mu \gg \nu^2$, Johnson [3] showed that the shock front approaches asymptotically the KdV soliton given by (9) with $\nu = 0$ and $u(\pm\infty) = 0$, i.e.,

$$u(s) = \tfrac{3}{2}\,\mathrm{sech}^2\,[s/2(\mu)^{1/2}]. \tag{17}$$

It should be noticed that the soliton (17) propagates with the same velocity $c = 1$ (see (8)) as the KdVB shock. For $\nu^2/4\mu$ small but finite, the KdVB shocks to the right approach the periodic cnoidal wave solution of the KdV equation [3, 10] during an increasingly large distance as $\nu^2/4\mu$ decreases (see Figs. 2 and 3). These statements are made clear by the numerical solutions of the KdVB equation shown in Section 3.

3. Numerical Experiments

The numerical solution of (1) subject to the boundary conditions (2a) and (2b) was carried out with the accurate space derivative method (ASD) [11, 12]. In this method, $u(x, t + \Delta t)$ is computed from $u(x, t)$ by a Taylor series

$$u(t + \Delta t) \approx u(t) + \frac{\partial u(t)}{\partial t}\Delta t + \frac{\partial^2 u(t)}{\partial t^2}\frac{\Delta t^2}{2} + \frac{\partial^3 u(t)}{\partial t^3}\frac{\Delta t^3}{6}. \tag{18}$$

The time derivatives in (18) are computed by successive differentiation using (1):

$$\frac{\partial u}{\partial t} = -2u\frac{\partial u}{\partial x} + \nu\frac{\partial^2 u}{\partial x^2} - \mu\frac{\partial^3 u}{\partial x^3}, \tag{19}$$

$$\frac{\partial^2 u}{\partial t^2} = -2\frac{\partial u}{\partial t}\frac{\partial u}{\partial x} - 2u\frac{\partial}{\partial x}\left(\frac{\partial u}{\partial t}\right) + \nu\frac{\partial^2}{\partial x^2}\left(\frac{\partial u}{\partial t}\right) - \mu\frac{\partial^3}{\partial x^3}\left(\frac{\partial u}{\partial t}\right), \tag{20}$$

$$\frac{\partial^3 u}{\partial t^3} = -2\frac{\partial^2 u}{\partial t^2}\frac{\partial u}{\partial x} - 4\frac{\partial u}{\partial t}\frac{\partial}{\partial x}\left(\frac{\partial u}{\partial t}\right) - 2u\frac{\partial}{\partial x}\left(\frac{\partial^2 u}{\partial t^2}\right) + \nu\frac{\partial^2}{\partial x^2}\left(\frac{\partial^2 u}{\partial t^2}\right) - \mu\frac{\partial^3}{\partial x^3}\left(\frac{\partial^2 u}{\partial t^2}\right). \tag{21}$$

The x-derivative terms in (19)–(21) are computed by Fourier methods. Let $U(k, t)$ be the finite Fourier transform of $u(x, t)$ defined over the computational domain [13]. The lth-order derivative of $u(x, t)$ is then given by

$$(\partial^l u/\partial x^l) = \sum_k (ik)^l\, U(k, t)\exp(ikx), \tag{22}$$

where $i = (-1)^{1/2}$ and the summation in (22) is carried out for all wavenumbers k which can be represented over the computational mesh. This method of computing the space derivatives gives results which are substantially more accurate than those obtained from finite difference expressions. The procedures used in order to satisfy numerically the boundary conditions (2a) and (2b) as well as the stability analysis of the numerical method are discussed in [11].

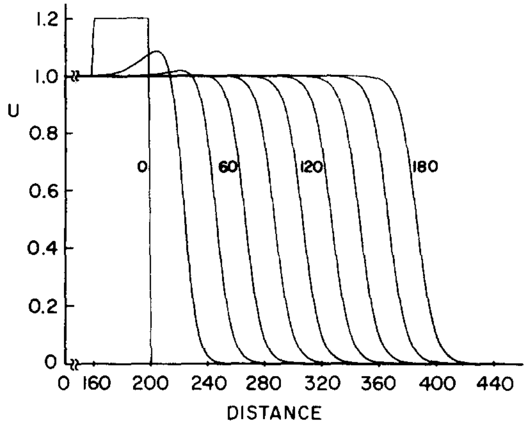

FIG. 1. Evolution of nonanalytic initial data, a step function with a large superimposed local perturbation, into a monotonic shock. The time separation between any two successive plots is 20 time units; the numbers on the curves are values of time. The upstream value is one, giving a shock speed of unity, as can be seen by inspection. The dispersion and diffusion coefficients are $\mu = 1$ and $\nu = 6$. The quantitative agreement with the asymptotic solution is shown in Table I.

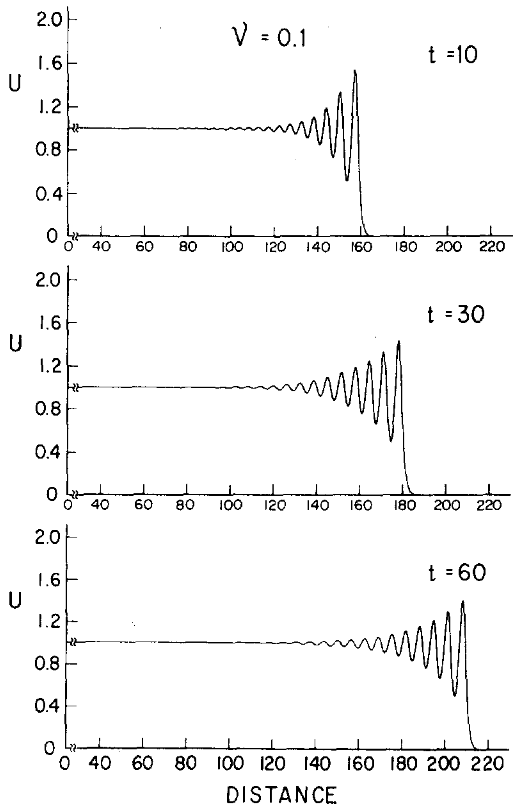

FIG. 2. Evolution of nonanalytic initial data, a step function, into an oscillatory shock. The upstream value is one, giving a shock speed of unity, as can be seen by inspection. At $t = 60$ the shock is fully developed (see Table II). The dispersion coefficient is $\mu = 1$.

In Fig. 1, we show the evolution of nonanalytic initial data in the form of a step function with a large local perturbation superimposed on it into the monotonic KdVB shock. In all the computations shown, the dispersion coefficient and the upstream value are unity (see (1) and (2a)), and therefore the shock speed is also unity (see (8)). Note that the value of the diffusion coefficient ($\nu = 6$) satisfies well the condition (10). Figure 1 shows that the KdVB shock is fairly well established after 60 time units. As the separation between successive plots is 20 time units, the distance between them is also 20 length units, as can be seen by inspection; this shows clearly that the shock propagation speed is unity, as predicted.

The computation in Fig. 1 indicates that initial data satisfying the boundary conditions evolve asymptotically into a monotonic shock whose profile is determined uniquely by the parameters ν and μ (see (1)), and by the boundary conditions (2a) and (2b). The fact that there are no numerical stability problems whatever, even after 8,000 time

TABLE I

Comparison of Asymptotic with Numerical Results for the Monotonic Shock of Diffusion Coefficient $\nu = 6$[a]

	$u(s)$		
	Asymptotic		
s	First order	Second order	Computed at $t = 160$[b]
−30.63	0.994	0.995	0.994
−26.63	0.988	0.989	0.989
−22.63	0.977	0.979	0.979
−18.63	0.957	0.960	0.960
−14.63	0.920	0.924	0.924
−10.63	0.855	0.860	0.860
−6.63	0.751	0.757	0.757
−4.63	0.684	0.690	0.689
−2.63	0.608	0.613	0.613
−0.63	0.526	0.532	0.532
1.37	0.443	0.449	0.449
3.37	0.363	0.369	0.369
5.37	0.290	0.296	0.296
7.37	0.226	0.232	0.232
11.37	0.131	0.136	0.135
15.37	0.0716	0.0756	0.0754
19.37	0.0381	0.0409	0.0408
23.37	0.0199	0.0217	0.0217
27.37	0.0103	0.0115	0.0114
31.37	0.00533	0.00602	0.00599

[a] The wave profile amplitude $u(s)$ is given as a function of distance, which in the wave frame is measured with respect to the point of inflection of the wave.

[b] This profile was obtained after 8,000 time steps of computation, in single precision.

steps of computation in single precision, is a strong indication that the shock is physically stable also.

In Table I, we compare the numerical results at $t = 160$ (which required 8,000 time steps of computation in single precision) with the first- and second-order asymptotic solutions given by (14). The excellent agreement obtained indicates the high accuracy of the ASD method and of the asymptotic solution. It is noted that the first-order solution gives two-figure accuracy except at the right tail, while the second-order solution gives uniformly three-figure accuracy.

In Fig. 2 we show the oscillatory shock obtained when the diffusion and dispersion coefficients ($\nu = 0.1$ and $\mu = 1$) are chosen so as to satisfy criterion (11). The initial datum used was a step function. Although the step function is different from the initial data used in the computation shown in Fig. 1, the fact remains that the step function greatly differs from the steady-state profile of the oscillatory shock, and can thus be considered a very large perturbation of the steady waveform. A comparison of the

TABLE II

Comparison of Time-dependent and Time-independent Numerical Results for the Oscillatory Shock of Diffusion Coefficient $\nu = 0.1$[a]

Peak position		Peak height	
Time-dependent, computed at $t = 60$[b]	Time-independent	Time-dependent, computed at $t = 60$[b]	Time-independent
0	0	1.41	1.42
6.9	6.9	1.30	1.31
13.5	13.5	1.22	1.23
19.9	19.9	1.16	1.17
26.3	26.3	1.12	1.13
32.6	32.6	1.09	1.09
39.0	38.9	1.06	1.07
45.3	45.2	1.04	1.05
51.6	51.5	1.03	1.04
57.9	57.8	1.02	1.03
64.2	64.0	1.02	1.02
70.6	70.3	1.01	1.01
76.9	76.6	1.01	1.01
83.3	82.9	1.00	1.01
89.7	89.2	1.00	1.00
96.0	95.5	1.00	1.00
102.3	101.8	1.00	1.00

[a] The peak positions are measured relative to the highest peak.

[b] This oscillatory shock profile was obtained after 12,000 time steps of computation, in single precision.

oscillatory shock evolved after 60 time units with the numerical solution of the time-independent boundary value problem (9) [3] indicates that at $t = 60$ the shock is fully developed (see Table II). As before in Fig. 1, inspection of Fig. 2 indicates that the distance traveled by the shock front equals the time separation of the successive plots, showing that, even before it is fully developed, the shock propagates with the theoretically predicted speed of unity. One interesting observation is that initially the peak amplitude of the front overshoots the amplitude of the KdV soliton, 1.5 (see (17)), and that the amplitude of the successive peaks decays rather fast with distance. As the shock develops fully, the peak amplitude of the front becomes, as predicted by the phase-plane analysis [2, 3] smaller than the amplitude of the KdV soliton, 1.5 (see Table II); also, the amplitude of the successive peaks decays more slowly with distance.

The qualitative features revealed in the computation of Fig. 2 are shown more sharply in Fig. 3, a computation with $\nu = 0.05$ and $\mu = 1$. As the diffusion coefficient is half that of Fig. 2, the damping decreases greatly and the shock becomes much more

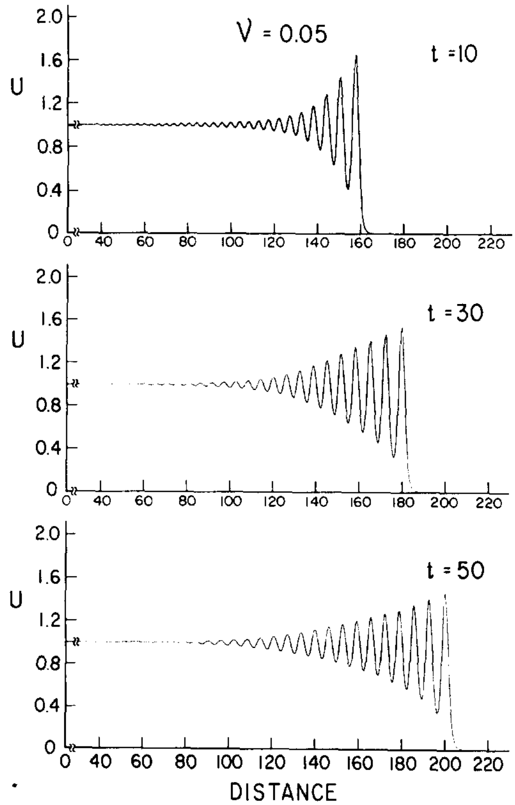

FIG. 3. Evolution of nonanalytic initial data, a step function, into a highly oscillatory shock. The shock speed is unity as in the previous cases. At $t = 50$, the shock is almost fully developed (see Table III). The dispersion coefficient is $\mu = 1$.

oscillatory. The first plot of Fig. 3 indicates that initially the peak amplitude of the front overshoots considerably the KdV soliton amplitude 1.5. The amplitude of the successive peaks decays rather sharply with distance. As the shock develops, the peak amplitude of the front becomes smaller, and the amplitude of the successive peaks decays also more slowly with distance. The computation shown in Fig. 3 was terminated at $t = 50$ for economy reasons. The comparison shown in Table III with the time-independent numerical results for the shock profile indicates that at $t = 50$ the shock is almost, although not quite, fully developed. The peak amplitude of the front has already decreased below the upper limit given by the KdV soliton amplitude, 1.5. A comparison of the last plots of Figs. 2 and 3 shows clearly that as ν decreases the oscillatory train of the shock damps more slowly with distance. This indicates that for very small but finite ν, the oscillatory train of the shock would approach

TABLE III

Comparison of Time-dependent and Time-independent Numerical Results for the Oscillatory Shock of Diffusion Coefficient $\nu = 0.05$[a]

Peak position		Peak height	
Time-dependent, computed at $t = 50$[b]	Time-independent	Time-dependent, computed at $t = 50$[b]	Time-independent
0	0	1.47	1.46
7.4	7.4	1.41	1.40
14.4	14.3	1.36	1.34
21.2	21.0	1.31	1.29
27.8	27.5	1.27	1.25
34.4	34.0	1.24	1.22
40.9	40.4	1.21	1.19
47.4	46.8	1.18	1.16
53.9	53.2	1.15	1.14
60.4	59.5	1.12	1.12
66.8	65.8	1.10	1.10
73.2	72.1	1.08	1.09
79.5	78.4	1.06	1.07
85.8	84.7	1.04	1.06
92.0	91.0	1.03	1.05
98.1	97.3	1.02	1.05
104.1	103.6	1.02	1.04
110.1	109.9	1.01	1.03
116.0	116.2	1.01	1.03
121.8	122.5	1.00	1.02

[a] The peak positions are measured relative to the highest peak.

[b] This oscillatory shock profile was obtained after 10,000 time steps of computation, in single precision.

along a certain distance the undamped periodic cnoidal wave solution of the KdV equation. This is, of course, as predicted by the phase-plane analysis [2, 3, 10].

We conclude by pointing out that, in the absence of time-dependent analytic results with which to compare the numerical solutions, we are not able to guarantee that the numerical experiments shown give the correct transient behavior of the solution. The greatest value of these computations is that they indicate that the numerical solutions evolve into the steady-state shocks predicted by the time-independent analysis. Because the initial data were chosen quite different from the shock profiles, the computation time necessary for the development of the shocks is quite large (more than 8,000 time steps); therefore, we feel that the absence of any numerical instability problems is, in itself, a strong indication of the physical stability of the shocks.

Acknowledgment

We are greatly indebted to Professor R. S. Johnson of the University of Newcastle upon Tyne for having given us listings of his computer programs for the solution of Eq. (9).

References

1. C. H. Su and C. S. Gardner, *J. Math. Phys. (N.Y.)* **10** (1969), 536.
2. H. Grad and P. N. Hu, *Phys. Fluids* **10** (1967), 2596.
3. R. S. Johnson, *J. Fluid Mech.* **42** (1970), 49.
4. R. S. Johnson, *Phys. Fluids* **15** (1972), 1963.
5. P. N. Hu, *Phys. Fluids* **15** (1972), 854.
6. J. D. Cole, *Quart. Appl. Math.* **9** (1951), 225.
7. E. Hopf, *Comm. Pure Appl. Math.* **3** (1950), 201.
8. P. Lax, *Comm. Pure Appl. Math.* **21** (1968), 467.
9. J. Canosa, *IBM J. Res. Develop.* **17** (1973), 307.
10. A. Jeffrey and T. Kakutani, *SIAM Review* **14** (1972), 582.
11. J. Gazdag, *J. Computational Phys.* **13** (1973), 100.
12. J. Gazdag and J. Canosa, *J. Appl. Probability* **11** (1974), 445.
13. E. Oran Brigham, "The Fast Fourier Transform," Prentice–Hall, Englewood Cliffs, N.J., 1974.